Long range order and two-fluid behavior in heavy electron materials

Kent R. Shirer[a], Abigail C. Shockley[a], Adam P. Dioguardi[a], John Crocker[a], Ching H. Lin[a], Nicholas apRoberts-Warren[a], David M. Nisson[a], Peter Klavins[a], Jason C. Cooley[b], Yi-feng Yang[c], and Nicholas J. Curro[a,1]

[a]Department of Physics, University of California, Davis, CA 95616; [b]Los Alamos National Laboratory, Los Alamos, NM 87545; and [c]Beijing National Laboratory for Condensed Matter Physics and Institute of Physics, Chinese Academy of Sciences, Beijing 100190, China

AUTHOR SUMMARY

Heavy-fermion compounds are special metals containing a lattice of localized magnetic moments whose hybridization with the background conduction electrons (see Fig. P1) gives rise to a new quantum state of matter: the heavy-electron Kondo liquid (1, 2). The properties of the Kondo liquid may be determined by combining nuclear magnetic resonance (NMR) Knight shift experiments (the nuclear spin resonance frequency shift arising from the electronic susceptibility) with measurements of the static magnetic susceptibility (3). Below a characteristic temperature the Kondo liquid coexists with the lattice of hybridized local moments, and their subsequent evolution is described phenomenologically by a two-fluid model. However, until the recent work of Yang and Pines (4), we lacked a framework that connects that emergent behavior to the development of ordered states at low temperatures. Here we report detailed new Knight shift measurements for several heavy-electron compounds that confirm the connection they propose between the hybridization strength and emergence of low-temperature order. The measurements provide detailed information on the ordered states of the Kondo liquid in several key heavy fermions and suggest that for weakly hybridizing materials, the approach to a local-moment ground state is always preceded by relocalization.

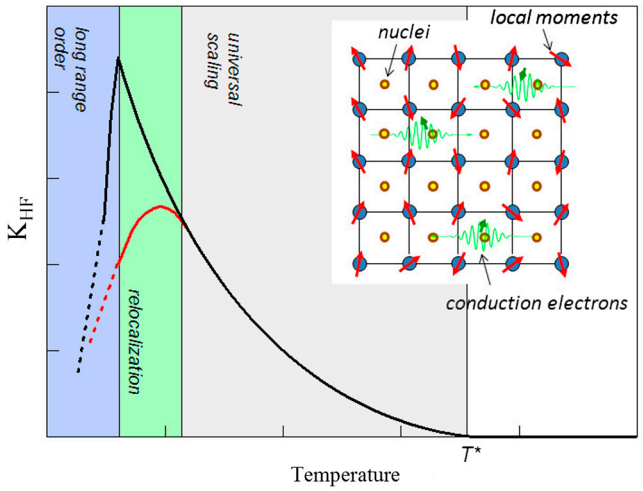

Fig. P1. The growth of the heavy-electron fluid susceptibility below a temperature T^* in the universal scaling regime. In some cases the susceptibility continues to grow until the onset of long-range order (black line); in other cases the local moments relocalize prior to ordering magnetically (red line). (*Inset*) Heavy-fermion compounds contain a lattice of local electrons and a sea of conduction electrons. Nuclear spins couple to both types of electrons, enabling one to measure the heavy-electron fluid component independently.

The interaction between the local moments and conduction electrons in heavy-fermion compounds is sufficiently weak such that at room temperature these two degrees of freedom behave independently of one another. Below a crossover temperature, T^*, the localized and conduction electrons begin to collectively hybridize, giving rise to a fluid of itinerant electrons with an enhanced effective mass (2). This behavior is reflected in various experimental quantities such as the electrical resistivity or magnetic susceptibility. NMR Knight shift measurements offer the most direct probe of the emergent behavior. The nuclear spins of the atoms in these materials experience hyperfine couplings to both the local-moment spin and conduction electron spins (3). In general, these two coupling constants differ from one another, which enables one to measure the magnetic susceptibility independently of the emergent heavy-electron fluid. NMR is the key to separating the contribution from the remaining local moments, which dominate the bulk magnetic susceptibility.

We have measured the NMR Knight shift of the heavy-electron fluid in several key materials in order to probe the emergence below T^* and the influence of long-range order at low temperatures. The heavy-fermion compounds $CeCoIn_5$ and $CeIrIn_5$ are prototypical heavy electron superconductors in which hybridization begins at temperatures well above the superconducting transition. Between these two temperatures, the local moments gradually dissolve into the heavy-electron fluid, and the heavy-electron susceptibility increases monotonically as a function of a universal scaling function of T/T^*. This behavior is common to all known heavy-fermion compounds, and only the onset temperature T^* changes from one material to the next. At the superconducting transition temperature, the susceptibility of the heavy-electron fluid drops suddenly, indicating that the superconducting condensate forms out of the heavy electrons (see Fig. P1). The universal scaling persists down to the transition temperature with no evidence of any precursor effects.

We find remarkably similar behavior in URu_2Si_2 at the so-called hidden-order transition temperature. This material has been investigated for more than 20 years and is known to undergo a phase transition at 17.5 K to a state that is not a conventional form of magnetic order (5). The ordered phase is usually referred to as hidden order, because the nature of this phase remains unclear at present. Our data reveals that the universal scaling persists from T^* down to the hidden-order

Author contributions: P.K., and N.J.C. designed research; K.R.S., A.C.S., A.P.D., J.C., C.H.L., N.a.-W., D.M.N., and J.C.C. performed research; K.R.S., A.C.S., Y.-f.Y., and N.J.C. analyzed data; and N.J.C. wrote the paper.

The authors declare no conflict of interest.

This article is a PNAS Direct Submission.

See Commentary on page 18241.

[1]To whom correspondence should be addressed. E-mail: curro@physics.ucdavis.edu.

See full research article on page E3067 of www.pnas.org.

Cite this Author Summary as: PNAS 10.1073/pnas.1209609109.

temperature. Below this temperature, the susceptibility drops and saturates at a finite value. This behavior suggests that the hidden order develops as a result of an instability of the itinerant heavy-electron fluid in a manner similar to the development of heavy-electron superconductivity.

In contrast to a monotonic increase of hybridization with decreasing temperature, compounds with magnetic ground states exhibit a relocalization of the local moments prior to the development of long-range order. At a temperature between the hybridization temperature and the magnetic ordering transition temperature, the heavy-electron susceptibility exhibits a downturn, indicating that hybridization of the local moments with the conduction electrons reverses its course and is suppressed (see Fig. P1). The ground state that results is not an instability of the hybridized heavy-electron fluid but rather long-range order of the local-moment electron spins. The degree to which the system has hybridized at the transition temperature may vary, in which case the magnitude of the ordered moments can be different from one material to the other.

These findings are important because they elucidate the interplay between the local moments, the heavy-electron fluid, and the nature of the ground state in heavy-electron materials. Not only do they provide us with a more comprehensive interpretation of experimental data, but we now can quantify and correlate the degree of hybridization in various materials with the long range order. Despite their low transition temperatures, heavy-electron superconductors are a model system for research on unconventional superconductivity. Our results suggest that many of the unusual phenomena that they exhibit should be interpreted in light of the two-fluid picture.

1. Yang Y-F, Pines D (2008) Universal behavior in heavy-electron materials. *Phys Rev Lett* 100:096404.
2. Yang Y-F, Fisk Z, Lee H-O, Thompson JD, Pines D (2008) Scaling the kondo lattice. *Nature* 454:611–613.
3. Curro NJ, Young BL, Schmalian J, Pines D (2004) Scaling in the emergent behavior of heavy-electron materials. *Phys Rev B* 70:235117.
4. Yang Y-F, Pines D (2012) Emergent states in heavy electron materials. *Proc Natl Acad Sci USA* 45:3060–3066.
5. Mydosh JA, Oppeneer PM (2011) Colloquium: Hidden order, superconductivity, and magnetism: The unsolved case of URu_2Si_2. *Rev Mod Phys* 83:1301–1322.

Long range order and two-fluid behavior in heavy electron materials

Kent R. Shirer[a], Abigail C. Shockley[a], Adam P. Dioguardi[a], John Crocker[a], Ching H. Lin[a], Nicholas apRoberts-Warren[a], David M. Nisson[a], Peter Klavins[a], Jason C. Cooley[b], Yi-feng Yang[c], and Nicholas J. Curro[a,1]

[a]Department of Physics, University of California, Davis, CA 95616; [b]Los Alamos National Laboratory, Los Alamos, NM 87545; and [c]Beijing National Laboratory for Condensed Matter Physics and Institute of Physics, Chinese Academy of Sciences, Beijing 100190, China

Edited by Malcolm R. Beasley, Stanford University, Stanford, CA, and approved August 31, 2012 (received for review June 12, 2012)

The heavy electron Kondo liquid is an emergent state of condensed matter that displays universal behavior independent of material details. Properties of the heavy electron liquid are best probed by NMR Knight shift measurements, which provide a direct measure of the behavior of the heavy electron liquid that emerges below the Kondo lattice coherence temperature as the lattice of local moments hybridizes with the background conduction electrons. Because the transfer of spectral weight between the localized and itinerant electronic degrees of freedom is gradual, the Kondo liquid typically coexists with the local moment component until the material orders at low temperatures. The two-fluid formula captures this behavior in a broad range of materials in the paramagnetic state. In order to investigate two-fluid behavior and the onset and physical origin of different long range ordered ground states in heavy electron materials, we have extended Knight shift measurements to URu_2Si_2, $CeIrIn_5$, and $CeRhIn_5$. In $CeRhIn_5$ we find that the antiferromagnetic order is preceded by a relocalization of the Kondo liquid, providing independent evidence for a local moment origin of antiferromagnetism. In URu_2Si_2 the hidden order is shown to emerge directly from the Kondo liquid and so is not associated with local moment physics. Our results imply that the nature of the ground state is strongly coupled with the hybridization in the Kondo lattice in agreement with phase diagram proposed by Yang and Pines.

nuclear magnetic resonance | heavy fermion | hyperfine couplings

Competition between different energy scales gives rise to a rich spectrum of emergent ground states in strongly correlated electron materials. In the heavy fermion compounds, a lattice of nearly localized f electrons interacts with a sea of conduction electrons, and depending on the magnitude of this interaction different types of long-range order may develop at low temperatures (1). The Kondo lattice model strives to capture the essential physics of heavy fermion materials by considering the various magnetic interactions between the conduction electron spins, S_c, and the local moment spins, S_f (2). Different ground states can emerge depending on the relative strengths of the interaction, J, between S_c and S_f and the intersite interaction, J_{ff}, between the S_f spins (3, 4). Much of the physics of the phase diagram is driven by a quantum critical point, which separates long-range ordered ground states from those in which the local moments have fully hybridized with the conduction electrons to form itinerant states with large effective masses and large Fermi surfaces (5). In several materials quantum critical fluctuations give rise to anomalous non-Fermi liquid behavior in various bulk transport and thermodynamic quantities (6–8).

In recent years, evidence has emerged that in the high temperature disordered phase the electronic degrees of freedom simultaneously exhibit both itinerant and localized behavior (9). Below a temperature T^* that marks the onset of hybridization or lattice coherence, several experimental quantities exhibit a temperature dependence that is well described by a fluid of hybridized heavy quasiparticles coexisting with partially screened local moments (3, 10). In the two-fluid picture, the transfer of spectral weight from the local moments to the heavy electrons is described by a quantity $f(T)$ (10). Above a temperature T^*, the local moments and conduction electrons remain uncoupled. Below T^* the local moments gradually dissolve into the hybridized heavy electron fluid as the temperature is lowered. This crossover can be measured directly via nuclear magnetic resonance (NMR) Knight shift experiments (11). The contribution to the Knight shift from the heavy electrons, K_{HF}, exhibits a universal logarithmic divergence with decreasing temperature below T^* in the paramagnetic state. In superconducting $CeCoIn_5$ this scaling persists down to T_c indicating that the condensate emerges from the heavy electron degrees of freedom (12). Relatively little is known, however, about how this scaling behaves in materials with other types of ordered ground states. Here we report Knight shift data in both URu_2Si_2 and $CeRhIn_5$. In the former the scaling persists down to the onset of hidden order at T_{HO}; but in the latter the heavy electron spectral weight reverses course and the local moments relocalize above the Neel temperature, T_N, similar to the antiferromagnet $CePt_2In_7$ (13). These results imply generally that the heavy electron fluid is either unstable to a Fermi surface instability such as hidden order or superconductivity or collapses to form ordered local moments.

Knight Shift Anomalies

The Zeeman interaction of an isolated nuclear spin $\hat{\mathbf{I}}$ in an external magnetic field $\mathbf{H}_0$ is given by $\mathscr{H}_Z = \gamma\hbar\hat{\mathbf{I}}\cdot\mathbf{H}_0$, where γ is the gyromagnetic ratio and $\hbar$ is the reduced Planck constant. In this case the nuclear spin resonance frequency is given by the Larmor frequency $\omega_L = \gamma H_0$. In condensed matter systems the nuclear spins typically experience a hyperfine coupling to the electron spins, $\mathscr{H}_{\rm hyp} = \gamma\hbar g\mu_B\hat{\mathbf{I}}\cdot\mathbf{A}\cdot\mathbf{S}$, where $\mathbf{S}$ is the electron spin, $\mathbf{A}$ is the hyperfine coupling g is the g-factor and μ_B is the Bohr magneton. The hyperfine coupling is in general a tensor that depends on the details of the bonding and quantum chemistry of the material of interest. $\mathbf{S}$ can be the unpaired spin moment of an unfilled shell, the net conduction electron spin of a Fermi sea polarized by a magnetic field, or the spin-orbit coupled moment of a localized electron. $\mathbf{S}$ may or may not be located on the same ion as the nuclear moment; the former is referred to as on-site coupling and the latter is transferred coupling. In the paramagnetic state the electron spin is polarized by the external field $\mathbf{S} = \chi\cdot\mathbf{H}_0/g\mu_B$, where χ is the susceptibility. Thus the nuclear spin experiences an effective Hamiltonian:

$$\mathscr{H}_Z + \mathscr{H}_{\rm hyp} = \gamma\hbar\hat{\mathbf{I}}\cdot(\mathbf{1}+\mathbf{K})\cdot\mathbf{H}_0, \qquad [1]$$

Author contributions: P.K. and N.J.C. designed research; K.R.S., A.C.S., A.P.D., J.C., C.H.L., N.a.-W., D.M.N., and J.C.C. performed research; K.R.S., A.C.S., Y.-f.Y., and N.J.C. analyzed data; and N.J.C. wrote the paper.

The authors declare no conflict of interest.

This article is a PNAS Direct Submission.

See Commentary on page 18241.

[1]To whom correspondence should be addressed. E-mail: curro@physics.ucdavis.edu.

See Author Summary on page 18249 (volume 109, number 45).

where the Knight shift tensor $\mathbf{K} = \mathbf{A} \cdot \chi$ is unit-less. The resonance frequency is given by $\omega = \omega_L(1 + K(\theta, \phi))$, where $K(\theta, \phi) = \mathbf{H}_0 \cdot \mathbf{A} \cdot \chi \cdot \mathbf{H}_0 / H_0^2$ depends on the polar angles θ and ϕ that describe the relative orientation of the field with respect to the principal axes of the Knight shift tensor. For the isotropic case the shift $K = A\chi$ is independent of direction. Strictly speaking the Knight shift was originally defined as the paramagnetic shift from the Pauli susceptibility in metals but in practice refers to any shift K arising from the electronic susceptibility.

The magnetic susceptibility and the Knight shift can be measured independently. One can extract the hyperfine coupling A by plotting the Knight shift versus the susceptibility with temperature as an implicit parameter [such a plot is traditionally known as a Clogston–Jaccarino plot (14)]. If there is a single electronic spin component that gives rise to the magnetic susceptibility, then the Clogston–Jaccarino plot is a straight line with slope A and intercept K_0. K_0 is a temperature independent offset that is usually given by the orbital susceptibility and diamagnetic contributions (15).

Breakdown of Linearity and Failure of Local Pictures. All known heavy fermion materials exhibit a Knight shift anomaly where the Clogston–Jaccarino plot deviates from linearity below an onset temperature, T^* (11). This phenomenon is also visible in a plot comparing K and χ versus temperature, as seen in Fig. 1, where T^* marks the temperature below which K no longer tracks χ. This breakdown can arise from the presence of impurity phases, which contribute to the bulk susceptibility but not to the Knight shift. However, Knight shift anomalies occur ubiquitously in single phase highly pure heavy fermion materials and are intrinsic phenomena. Several different theories have been proposed to explain these anomalies. These theories generally fall into two categories: (*i*) a temperature dependent hyperfine coupling $A(T)$ or (*ii*) multiple spin degrees of freedom. It has been argued that A acquires a temperature dependence either because of Kondo screening (16) or because of different populations of crystal field levels of the 4f(5f) electrons in these materials (17). A major flaw in such an argument is that the hyperfine coupling is determined by large energy scales involving exchange integrals between different atomic orbitals, and because the Kondo and/or crystal field interactions are several orders of magnitude smaller they cannot give rise to large perturbations in the hyperfine couplings (18). Furthermore, in materials such as the $CeMIn_5$ system both the Knight shift anomaly and the crystalline electric field interaction are well characterized and are clearly uncorrelated (see Table 1) (19).

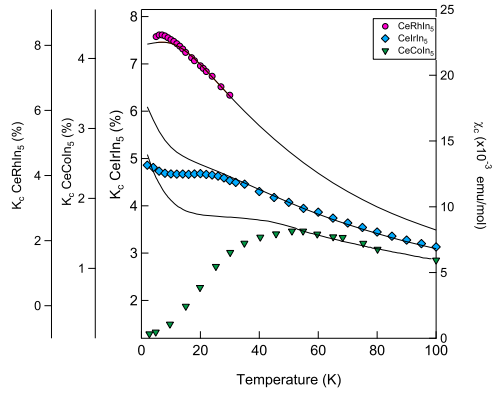

Fig. 1. The Knight shift (solid points) and the bulk susceptibility (solid lines) of the In(1) for field along the *c* direction in $CeMIn_5$ for M = Rh ,Ir and Co. T^* is the temperature where the two quantities no longer are proportional to one another, and is clearly material dependent. In some cases K appears to exceed χ and in others K decreases.

Table 1. Crystal field levels and coherence temperatures in the $CeMIn_5$ materials

Material	T^* (K)	Δ (K) (from ref. 19)
$CeCoIn_5$	42	100
$CeRhIn_5$	18(1)	80
$CeIrIn_5$	31(5)	78

Two Spin Components. Because Kondo lattice materials have both localized f electrons and itinerant conduction electrons, a theory that includes different hyperfine couplings to multiple spin degrees of freedom fits better. The two-fluid picture correctly predicts the temperature dependence of the Knight shift anomalies seen experimentally in heavy fermion materials. In the Kondo lattice model the local moment spins, $\mathbf{S}_f$ interact with a sea of conduction electron spins, $\mathbf{S}_c$ through a Kondo interaction:

$$\mathscr{H}_K = J \sum_i \mathbf{S}_f(\mathbf{r}_i) \cdot \mathbf{S}_c + \sum_{ij} J_{ff}(\mathbf{r}_{ij}) \mathbf{S}_f(\mathbf{r}_i) \cdot \mathbf{S}_f(\mathbf{r}_j) \qquad [2]$$

where the sums are over the lattice positions $\mathbf{r}_i$ of the localized f electrons. The general solution of the Kondo lattice has not been resolved to date, but the two-fluid description given by Nakatsuji, Fisk, Pines, and Yang provides a phenomenological framework to describe the phase diagram of the Kondo lattice problem (3, 4, 9, 10). This approach offers a natural interpretation of the NMR Knight shift anomaly in terms of two hyperfine couplings to the two different electron spins:

$$\mathscr{H}_{\text{hyp}} = \gamma \hbar g \mu_B \hat{\mathbf{I}} \cdot (A\mathbf{S}_c + B\mathbf{S}_f) \qquad [3]$$

where A and B are the hyperfine couplings to the conduction electron and local moment spins, respectively (11). The susceptibility is the sum of three contributions $\chi = \chi_{cc} + 2\chi_{cf} + \chi_{ff}$, where $\chi_{\alpha\beta} = \langle \mathbf{S}_\alpha \mathbf{S}_\beta \rangle$ with $\alpha, \beta = c, f$. In the paramagnetic state $\langle S_c \rangle = (\chi_{cc} + \chi_{cf}) H_0$ and $\langle S_f \rangle = (\chi_{ff} + \chi_{cf}) H_0$, thus the Knight shift is given by:

$$K = K_0 + A\chi_{cc} + (A + B)\chi_{cf} + B\chi_{ff}. \qquad [4]$$

The Knight shift weighs the different correlation functions separately than the total susceptibility, which leads to important consequences if the correlation functions have different temperature dependencies. $K \sim \chi$ if and only if $A = B$. If $A \neq B$, then the Clogston–Jaccarino plot will no longer be linear. By measuring K and χ independently, one can exploit this difference to extract linear combinations of these individual susceptibilities. No other experimental technique can access these susceptibilities.

Free Spin Model. The general solution for the susceptibilities $\chi_{\alpha\beta}$ of the Kondo lattice problem has not been solved to date. It is useful, however, to consider a simplified model. Consider the case of two free $S = \frac{1}{2}$ spins $\mathbf{S}_c$ and $\mathbf{S}_f$ that experience a Heisenberg coupling J. The Hamiltonian for this spin system in the presence of an external magnetic field $\mathbf{H}_0$ is given by:

$$\hat{\mathscr{H}} = g_c \mu_B \mathbf{S}_c \cdot \mathbf{H}_0 + g_f \mu_B \mathbf{S}_\mathbf{f} \cdot \mathbf{H}_0 + J\mathbf{S}_c \cdot \mathbf{S}_f, \qquad [5]$$

where μ_B is the Bohr magneton and $g_{c,f}$ are the g factors of the two different spins. This simplified model is clearly an incorrect physical description of the Kondo lattice problem where the spins are not free but part of a complex many-body problem involving the Fermi sea and various intersite interactions. This model is the simplest case, however, which captures the essence of the Knight shift anomaly and can be solved exactly.

The free energy is given by $F = -k_B T \ln Z$, where Z is the partition function; the susceptibility of the system is given by the second derivative of the free energy with respect to field:

$\chi = \frac{\partial^2 F}{\partial H^2}|_{H\to 0}$. The susceptibility is given as the sum of three contributions:

$$\chi_{cc}(x) = \left(\frac{g_c^2\mu_B^2}{4k_BT}\right)\frac{2(e^x + x - 1)}{(3 + e^x)x} \quad [6]$$

$$\chi_{ff}(x) = \left(\frac{g_f^2\mu_B^2}{4k_BT}\right)\frac{2(e^x + x - 1)}{(3 + e^x)x} \quad [7]$$

$$\chi_{cf}(x) = -\left(\frac{g_c g_f \mu_B^2}{4k_BJ}\right)\frac{2(e^x - x - 1)}{3 + e^x} \quad [8]$$

where $x = J/k_BT$. The temperature dependence of these three susceptibilities is shown in Fig. 2. In the high temperature limit ($T \gg J/k_B$) χ_{cc} and χ_{ff} exhibit Curie behavior and $\chi_{cf} \to 0$ as expected. For low temperature ($T \lesssim J/k_B$) the behavior is modified by the tendency to form a singlet ground state. As shown in Fig. 2 χ_{cc}, χ_{ff} and χ_{cf} change dramatically below $T \approx J/k_B$ and saturate at low temperatures. The Knight shift, given by Eq. **4**, is shown as well in Fig. 2. Clearly K tracks χ for $T \gg J/k_B$ but deviates below $T \approx J/k_B$, creating an anomaly in the Clogston–Jaccarino plot in Fig. 3. The breakdown of linearity arises because $|\chi_{cf}|$ increases below $T \approx J/k_B$ and has a different temperature dependence than χ_{cc} and χ_{ff}.

Two-Fluid Model. The three individual susceptibilities $\chi_{\alpha\beta}$ will exhibit different temperature dependencies in a Kondo lattice than the free spin model considered above. In particular, at high temperatures χ_{cc} is given by the temperature-independent Pauli susceptibility of the conduction electrons, and χ_{ff} is given by a Curie–Weiss susceptibility of the local moments. Therefore above a crossover temperature, T^*, χ_{ff} dominates and $K = K_0 + B\chi$. Below T^* χ_{cf} becomes significant and the growth of this component can be measured by the quantity $K_{HF} = K - K_0 - B\chi = (A - B)(\chi_{cf} + \chi_{cc})$. The two-fluid model postulates that K_{HF} is proportional to the susceptibility of the heavy electron fluid; its temperature dependence probes both growth of hybridization and its relative spectral weight (3, 10). Empirically it has been found that in the paramagnetic phase of a broad range of materials, $K_{HF}(T)$ varies as:

$$K_{HF}(T) = K_{HF}^0(1 - T/T^*)^{3/2}[1 + \log(T^*/T)] \quad [9]$$

where K_{HF}^0 is a constant (10). In other words, K_{HF} exhibits a universal scaling with the quantity T/T^*, where T^* and K_{HF}^0 are material-dependent quantities. K_{HF}^0 is proportional to A–B and can be either positive or negative. T^* agrees well with several other experimental measurements of the coherence temperature of the Kondo lattice (10). The Knight shift thus provides a direct probe of the susceptibility of the emergent heavy electron fluid in the paramagnetic state. There are, however, several pieces of missing information regarding the behavior of the heavy electron component that need to be addressed. For example, the Knight shift anomaly is strongly anisotropic in some materials, and it has not been clear whether this is an intrinsic feature of the heavy electron fluid or rather a reflection of the anisotropy of the hyperfine couplings (11). Furthermore, the Yang–Pines scaling works remarkably well for temperatures down to approximately 10% of T^*, but until recently there has been relatively little information about the evolution of the heavy electron fluid at lower temperature particularly when long-range order develops. We address both of these issues in turn below.

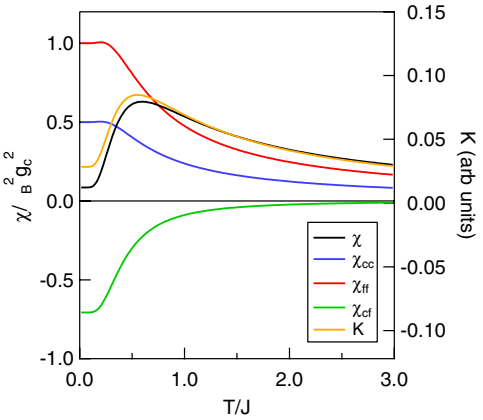

Fig. 2. The components of the magnetic susceptibility for the model spin system. The Knight shift begins to deviate from the bulk susceptibility below a temperature $T \approx J$. In this case, we have used $g_f/g_c = \sqrt{2}$, and $B/A = 1.5$. If $g_f = g_c$, then $\chi(T \to 0) \to 0$, as expected for a singlet ground state.

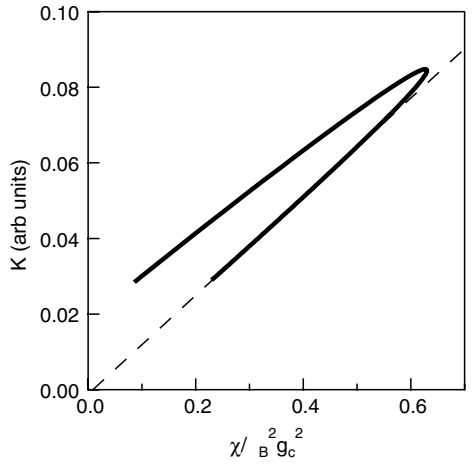

Fig. 3. Knight shift versus the bulk susceptibility for the model spin system with temperature as an implicit parameter. The Knight shift begins to deviate from the bulk susceptibility below a temperature $T \approx J/k_B$. In this case, we have used $g_f/g_c = \sqrt{2}$, and $B/A = 1.5$.

Anisotropy. One of the striking features of the emergence of the heavy electron component in Kondo lattice materials is the anisotropy of the Knight shift anomaly. For example, in $CeCoIn_5$ the Knight shift of the In(1) site exhibits a strong anomaly for $\mathbf{H}_0 \| c$ but no anomaly for $\mathbf{H}_0 \perp c$ (20). In order to probe this behavior in greater detail, we have measured the full Knight shift

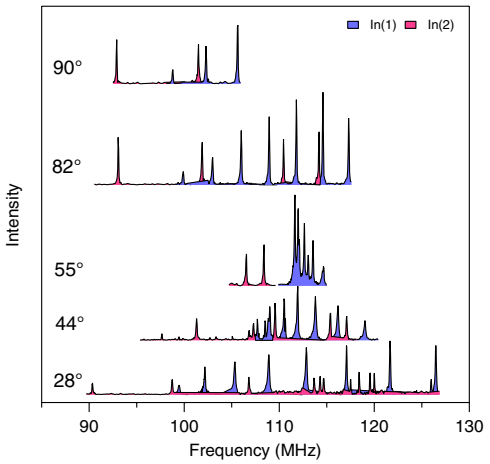

Fig. 4. Spectra of the In(1) and In(2) in $CeIrIn_5$ at 6 K and constant field of 11.7 T, where θ is the angle between the c axis and the field. There are multiple satellite transitions for each site due to the quadrupolar splitting (37).

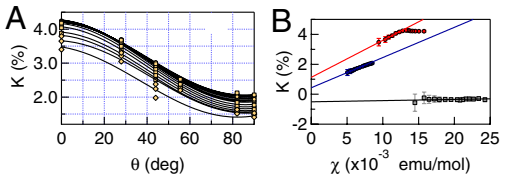

Fig. 5. (*A*) The Knight shift of the In(1) in $CeIrIn_5$ versus angle at several different temperatures. Solid points are fits to Eq. **4**. (*B*) K_{aa} (blue), K_{cc} (red) and K_{ac} (gray) versus χ_{aa}, χ_{cc} and $\chi_{aa}+\chi_{cc}$. Solid lines are linear fits as described in the text.

tensor in $CeIrIn_5$. $CeIrIn_5$ is isostructural to $CeCoIn_5$ and is a superconductor with $T_c = 0.4$ K. A single crystal grown in In flux was mounted in a custom-made goniometer probe, and the orientation of the c axis of the crystal was varied from 0 to 90 degrees. ^{115}In has spin $I = \frac{9}{2}$, and there are two different crystallographic sites for In in this material; consequently there are several different transitions as seen in Fig. 4. Spectra were obtained as a function of orientation and temperature, and the Knight shift was extracted after correcting for the quadrupolar shift of the resonance (21). Fig. 5 shows K versus θ, where θ is the angle between c and $\mathbf{H}_0$.

The strong angular dependence can be understood in terms of the tensor nature of the hyperfine coupling. For $T > T^*$ the tensor is given by

$$\mathbf{B} = \begin{pmatrix} B_{aa} & B_{ab} & B_{ac} \\ B_{ab} & B_{bb} & B_{bc} \\ B_{ac} & B_{bc} & B_{cc} \end{pmatrix} \qquad [10]$$

in the basis defined by the tetragonal unit cell with unit vectors a, b, and c; and the susceptibility tensor is

$$\chi = \begin{pmatrix} \chi_{aa} & 0 & 0 \\ 0 & \chi_{aa} & 0 \\ 0 & 0 & \chi_{cc} \end{pmatrix}. \qquad [11]$$

We therefore have

$$K(\theta) = K_{aa}\sin^2\theta + K_{cc}\cos^2\theta + K_{ac}\sin\theta\cos\theta \qquad [12]$$

where θ is the angle between $\mathbf{H}_0$ and the c-axis, $K_{aa} = K^0_{aa} + B_{aa}\chi_{aa}$, $K_{cc} = K^0_{cc} + B_{cc}\chi_{cc}$, and $K_{ac} = K^0_{ac} + B_{ac}(\chi_{aa}+\chi_{cc})$. The solid lines in Fig. 5*A* are fits to this equation, and Fig. 5*B* shows K_{aa}, K_{cc} and K_{ac} versus χ_{aa}, χ_{cc} , and $\chi_{aa}+\chi_{cc}$, respectively. The fitted values are given in Table 2. The solid lines are fits that yield the hyperfine couplings B_{aa}, B_{cc}, B_{ac} , and the orbital shifts K^0_{aa}, K^0_{cc} , and K^0_{ac}. The fact that $B_{ac} \approx 0$ within error bars implies that the principal axes of the hyperfine tensor coincide with those of the unit cell. On the other hand, $K^0_{ac} \neq 0$ implies that the orbital shift tensor is not diagonal in the crystal basis. Rather it is rotated by an angle of approximately 28° from the c direction, suggesting a possible role of directionality between the In 5p orbitals and the Ce 4f orbitals.

The emergence of the heavy fermion fluid is evident by computing $K_{HF}(\theta, T) = K(\theta, T) - K(\theta)$, where $K(\theta)$ is given by Eq. **12** and using the fitted parameters. This data in shown in Fig. 6 as well as fits to Eq. **9**, which give a value of $T^* = 31(5)$ K. From this data, it is clear that T^* does not vary as a function of angle, but rather the overall scale of the quantity K^0_{HF} decreases with angle until it reaches approximately zero by $\theta = 90°$. The angular dependence clearly indicates that $K_{HF}(\theta, T)$ does not simply vanish for the perpendicular direction but decreases gradually as a function of orientation in a continuous fashion. The constant K^0_{HF} is anisotropic, but T^* is not. In fact, $\mathbf{K}^0_{HF}$ is proportional to **A**–**B** and is therefore a tensor quantity itself, which is clearly seen in the angular dependence shown in the inset of Fig. 6. The solid line is a fit to $K^0_{HF} = K^0_{HF,c}\cos^2\theta + K^0_{HF,a}\sin^2\theta$. It is likely that the anisotropy arises primarily because of the hyperfine couplings, but it is not possible to rule out an additional contribution to the anisotropy from the quantity $\chi_{cf} + \chi_{cc}$. The fact that T^* does not depend on orientation suggests that the field $\mathbf{H}_0$ has little effect on the onset of coherence.

Superconducting Order

A key question in Kondo lattice materials is how the emergent heavy electron fluid and the remaining local moments interact to give rise to long range ordered states. Several materials exhibit a superconducting ground state, and it has long been assumed that the condensate forms from heavy electron quasiparticles. Recently we showed that this interpretation is supported by direct measurements of the Knight shift in the superconducting state (12). Fig. 7 displays $K(T)$ and $K_{HF}(T)$ for the In and Co sites in $CeCoIn_5$. Surprisingly, the total Knight shift $K(T)$ increases for some of the sites below T_c, and decreases for others. The normal expectation is that the spin susceptibility decreases below T_c in a superconductor because the Cooper pairs have zero spin. Application of the two-fluid analysis indicates that the heavy electron component, $K_{HF}(T)$, decreases as expected for a superconducting condensate. In fact, the data are best fit to a d-wave gap with value $\Delta(0) = 4.5\ k_B T_c$, in agreement with specific heat measurements. These results strongly suggest that the superconducting condensate arises as an instability of the heavy electron fluid.

Hidden Order

Another well-known heavy fermion system with long-range order at low temperature is URu_2Si_2, which exhibits a phase transition to a state with an unknown order parameter at $T_{HO} = 17.5$ K (22). This unusual phase has been studied for the past two decades and numerous theoretical order parameters have been proposed. Although the nature of the hidden order parameter remains unknown, extensive work has suggested that it has an itinerant nature and involves some type of Fermi surface instability (23). We have measured the Knight shift of the ^{29}Si in URu_2Si_2 in order to investigate the effect of hidden order on K_{HF}.

Polycrystalline samples of URu_2Si_2 were synthesized by arc melting in a gettered argon atmosphere, and an aligned powder was prepared in an epoxy matrix by curing a mixture of powder and epoxy in an external magnetic field of 9 T. Aligned powder samples are useful to enhance the surface-to-volume ratio and hence the NMR sensitivity. NMR measurements were carried out using a high homogeneity 500 MHz (11.7 T) Oxford Instruments magnet. The ^{29}Si($I = 1/2$) (natural abundance 4.6%) spectra were measured by spin echoes, and the signal-to-noise ratio was enhanced by summing several (approximately 100) echoes acquired via a Carr–Purcell–Meiboom–Gill pulse sequence (24). In this field, the hidden order transition is suppressed to 16 K (25). The spin lattice relaxation rate (T_1^{-1}) was measured as a function of the angle between the alignment axis and the mag-

Table 2. Measured hyperfine coupling constants in $CeIrIn_5$, $CeRhIn_5$, and URu_2Si_2

Material	site	B_{aa} (kOe/μ_B)	B_{cc} (kOe/μ_B)	B_{ac} (kOe/μ_B)	K^0_{aa} (%)	K^0_{cc} (%)	K^0_{ac} (%)
$CeIrIn_5$	In(1)	11.3(1)	13.8(1)	0.4(3)	1.1(2)	0.4(2)	−0.5(2)
$CeRhIn_5$	In(1)	-	21.4(5)	-	-	0.64(5)	-
URu_2Si_2	Si	-	4.3(1)	-	-	−0.07(1)	-

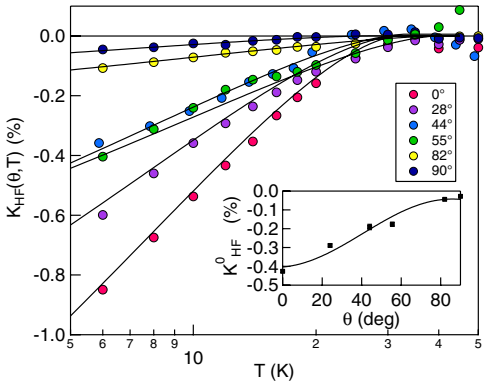

Fig. 6. The heavy electron component of the shift in $CeIrIn_5$ for the In(1) as a function of angle and temperature. The solid lines are fits to Eq. **9**. *Inset*: The fitted value K^0_{HF} versus angle. The solid line fit, described in the text, indicates the tensor nature of the hyperfine coupling **A**.

netic field $\mathbf{H}_0$ in order to properly align the sample, because T_1^{-1} is a strong function of orientation with a minimum for $\mathbf{H}_0 \| c$. Spectra are shown in Fig. 8, and the Knight shift along the c direction, K_c, is shown in Fig. 9. The total magnetic susceptibility, $\chi_c(T)$, is shown in Figs. 8 and 9 as a solid line. χ_c exhibited little or no field dependence in the temperature range of interest. The inset of Fig. 9 displays K_c versus χ. There is a clear anomaly that develops around 75 K, in agreement with previous data from Bernal. However, in contrast to previous measurements, we find that below T^* the Knight shift turns upward rather than downward (26).

In order to fit the Knight shift data and extract the temperature dependence of K_{HF}, we have fit both the K_c versus χ data and the K_{HF} versus T data simultaneously by minimizing the joint reduced $\chi^2(K_0, B, K^0_{HF}, T^*) = \chi^2_1(K_0, B) + \chi^2_2(K^0_{HF}, T^*)$. Individually, χ^2_1 and χ^2_2 provide the best fits to the two datasets, but because $K_{HF}(T)$ depends on K_0 and B, χ^2_2 is an implicit function of these fit parameters as well. The best fit is shown in the inset of Fig. 9. The fit parameters, listed in Table 2 are close to the

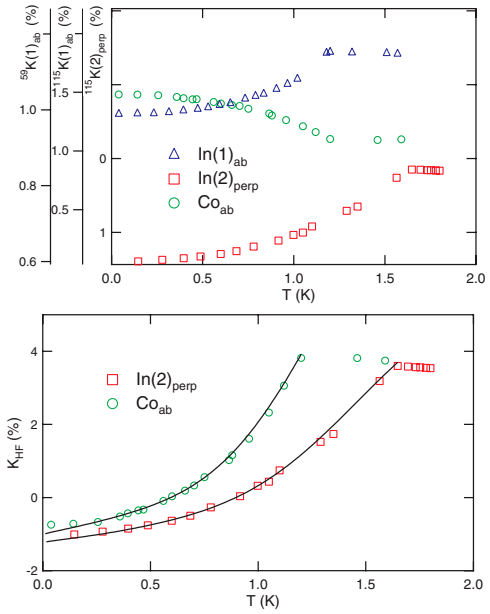

Fig. 7. (*Upper*) Knight shift of the In(1), In(2) and Co in $CeCoIn_5$ in the paramagnetic state for field in the *ab* plane. For In(2) there are two distinct crystallographic positions depending on the direction of the field. (*Lower*) The heavy electron susceptibility K_{HF} in the superconducting state. The solid lines are calculations as discussed in the text. Data are reproduced from ref. 12.

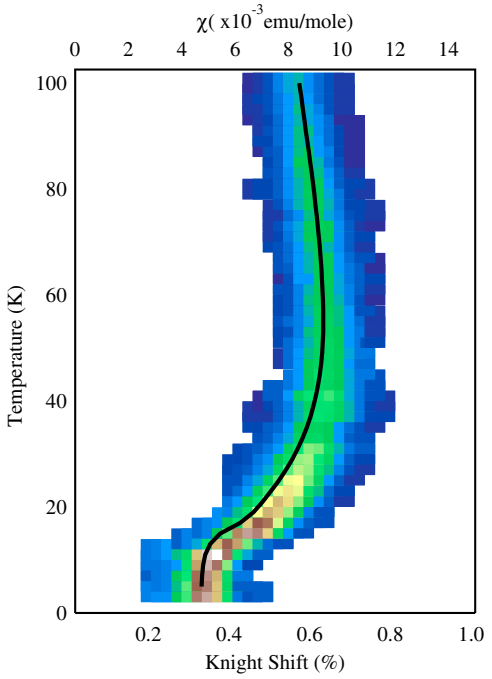

Fig. 8. Spectra of the ^{29}Si in URu_2Si_2 as a function of temperature. Color intensity (arb units) corresponds to the integral of the NMR spin echo. The solid black line is the bulk susceptibility.

values originally reported by Kohori (27). $K_{HF}(T)$ is shown in Fig. 10, and the best fit to Eq. **9** yields $T^* = 73(5)$ K. The data clearly indicate that $K_{HF}(T)$ grows monotonically down to the hidden ordering temperature at 16 K and is well described by the Yang–Pines scaling formula.

Because the f electrons in URu_2Si_2 are strongly hybridized at low temperatures, the Knight shift and the susceptibility recover a one-component picture below a delocalization temperature T_L (4). This allows us to determine the values of K_0, A and B. The susceptibility of the two components below T^* hence can be subtracted and the results are plotted in Fig. 11. The local component also follows the mean-field prediction for a hybridized spin liquid (4), $\chi_l \sim f_l/(T + T_l + f_l\theta)$, with $f_0 = 1.6$, $\theta = 175$ K given by the RKKY coupling and $T_l = 70$ K by local hybridization.

Below the hidden order transition temperature K_{HF} decreases dramatically and saturates at a value $\sim K_{HF}(T_{HO})/3$ at $T \sim 4$ K. This result suggests that, like the superconductivity in $CeCoIn_5$, the hidden order phase in URu_2Si_2 emerges from the itinerant heavy electron quasiparticles and is not a phenomenon associated with local moment physics (28). The partial suppression of K_{HF} is also consistent with specific heat measurements which indicate

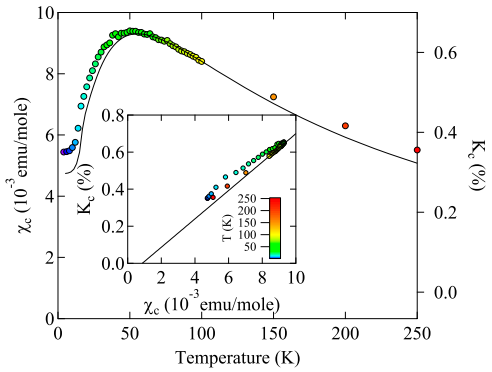

Fig. 9. The Knight shift of the Si (colored circles) and the susceptibility (solid line) in URu_2Si_2 for field along the c direction. The inset shows K versus χ.

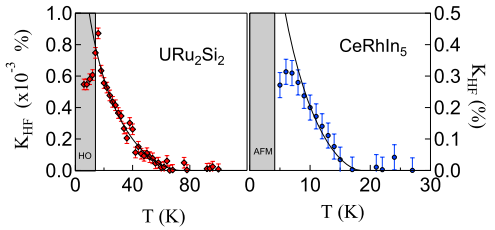

Fig. 10. $K_{HF}(T)$ versus T for URu_2Si_2 (left) and $CeRhIn_5$ (right). The solid black line are best fits to Eq. **9**. In URu_2Si_2 K_{HF} grows until the sudden onset of hidden order, whereas in $CeRhIn_5$ K_{HF} deviates from the scaling form below 8 K indicating the relocalization of the local moments.

that approximately 40% of the Fermi surface remains ungapped below the hidden order transition (29). Recent theoretical work has suggested the presence of a psuedogap in a range of 5–10 K above the hidden order transition (30). If one neglects the single outlying data point at 16 K, then the data may indicate a subtle change of scaling below approximately 23 K. However, we do not have sufficient precision to make any conclusive statements about the pseudogap.

The Knight shift anomaly K_{HF} below T_{HO} also follows the BCS prediction,

$$K_{\rm anom}(T) - K_{\rm anom}(0) \sim \int dE \left(-\frac{\partial f(E)}{\partial E}\right) N(E), \qquad [13]$$

where $f(E)$ is the Fermi distribution function and $N(E) = |E|/\sqrt{E^2 - \Delta(T)^2}$ is the density of states. The gap function $\Delta(T)$ has a mean-field temperature dependence,

$$\Delta(T) = \Delta(0)\tanh[2\sqrt{(T_{HO}/T - 1)}], \qquad [14]$$

where $\Delta(0) \sim 4.0\, k_B T_{HO}$ is the gap amplitude determined by STM experiments. We find a good fit to the Kondo liquid susceptibility below T_{HO} in Fig. 11.

Antiferromagnetism and Relocalization

In order to investigate the response of K_{HF} to long-range order we have measured the Knight shift of the ^{115}In(1) site in $CeRhIn_5$. $CeRhIn_5$ is an antiferromagnet at ambient pressure with an ordered moment of 0.4 μ_B and $T_N = 3.8$ K (31). Single crystals were grown in In flux using standard flux growth techniques. The $\frac{3}{2} \leftrightarrow \frac{1}{2}$ transition of the ^{115}In ($I = 9/2$) was observed for the In(1) by Hahn echoes, and the alignment of the crystal was confirmed by the splitting of the quadrupolar satellites (32). The Knight shift is shown in Fig. 12. There is a clear anomaly that develops at 17 K, in contrast to a previous report of 12 K (11). In this case the previous data consisted of only six data points over

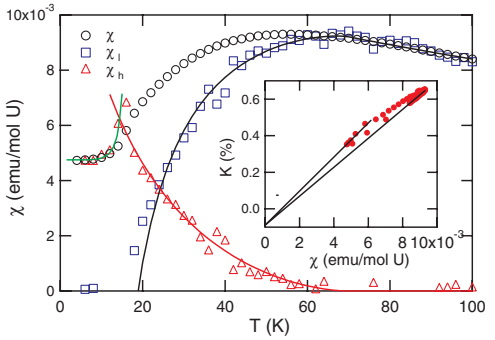

Fig. 11. Two-fluid analysis of the magnetic susceptibility in URu_2Si_2 by using the one-component behavior above T^* and below T_L. The solid lines are fit to the scaling formula of the Kondo liquid and the mean-field formula of the hybridized spin liquid for $T > T_{HO}$ and the Yosida function for $T < T_{HO}$ following the BCS prediction.

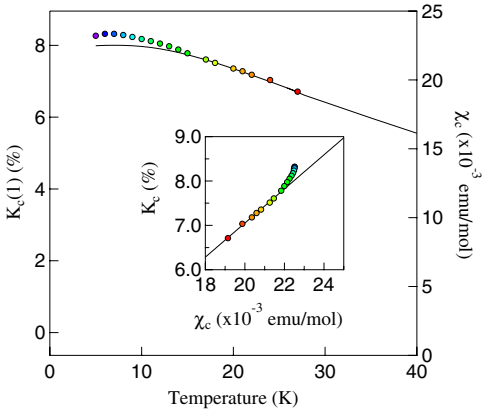

Fig. 12. The Knight shift of the In(1) (colored circles) and the susceptibility (solid line) in $CeRhIn_5$ for field along the c direction. The inset shows K versus χ.

a limited range and did not have the precision to discern the anomaly. By taking more data points at closely spaced intervals, we find K_c increases above the extrapolated value below T^*, in contrast to that in the $CeIrIn_5$ and $CeCoIn_5$ (see Fig. 1). The best fits to the data yield hyperfine couplings that are similar to those in $CeIrIn_5$ (see Table 2), and we find that $T^* = 18(1)$ K for $CeRhIn_5$.

The temperature dependence of the emergent heavy fermion component, $K_{HF}(T)$ is shown in Fig. 10*B* for $CeRhIn_5$. In contrast to the scaling behavior observed in $CeIrIn_5$, $CeCoIn_5$, and URu_2Si_2, K_{HF} does not follow the Yang–Pines scaling formula down to the ordering temperature, T_N. Rather, K_{HF} begins to deviate below 9 K, exhibits a maximum at 8 K and then decreases down to T_N. This temperature of the breakdown of scaling corresponds well with the onset of antiferromagnetic correlations observed by inelastic neutron scattering and NMR spin lattice relaxation measurements (33, 34). The physical picture that emerges is that the local moments begin to hybridize below T^*, but their spectral weight is only gradually transferred to the heavy electron fluid. At 9 K, the partially screened local moments begin to interact with one another and spectral weight is transferred back. This relocalization behavior was first observed in the antiferromagnet $CePt_2In_7$ (13). The fact that K_{HF} remains finite at T_N suggests that the ordered local moments still remain partially screened (4).

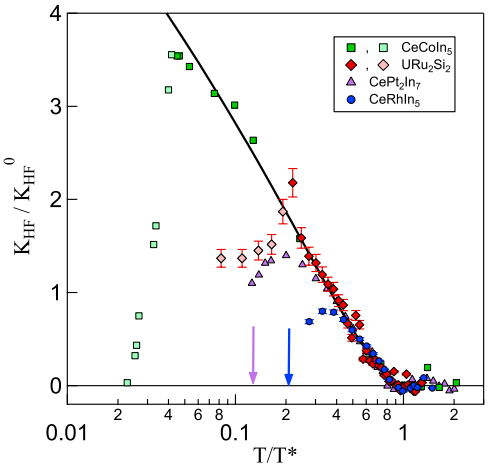

Fig. 13. $K_{HF}(T)$ (normalized) versus T/T^* for $CeCoIn_5$, $CePt_2In_7$, URu_2Si_2, and $CeRhIn_5$. Data points in the superconducting and hidden order states are lighter shades. The solid black line is Eq. **9**, and the vertical arrows indicate T_N for $CePt_2In_7$ and $CeRhIn_5$. Data for the $CeCoIn_5$ and $CePt_2In_7$ are reproduced from refs. 12 and 13.

It is interesting to compare the behavior of the heavy electron Knight shift observed in URu_2Si_2 and $CeRhIn_5$ with other Kondo lattice materials that undergo long-range order. Fig. 13 shows the scaled K_{HF} versus T/T^* for URu_2Si_2, $CeRhIn_5$, $CeCoIn_5$, and the antiferromagnet $CePt_2In_7$ ($T_N = 5.2$ K, $T^* \approx 40$ K) (11, 13). The onset of hybridization at T^* is identical for all the compounds, but the low temperature behavior depends critically on the ground state. In both $CeCoIn_5$ and URu_2Si_2 the spectral weight appears to be transferred continuously to the heavy electron fluid all the way down to the ordering temperature. Similar behavior is present in $CeIrIn_5$ ($T_c = 0.4$ K, not shown) down to 2 K. This behavior is surprising, because one might expect that the hidden order and/or superconductivity would emerge from a fully formed heavy electron state. Such a state would be characterized by a temperature independent K_{HF}, but that is clearly not the case for either material. In fact, the only known cases where K_{HF} appears to plateau at a constant value are $CeSn_3$ and $Ce_3Bi_4Pt_3$, neither of which exhibit long-range order (11).

The relocalization behavior in $CeRhIn_5$ and $CePt_2In_7$ contrasts starkly with that of the URu_2Si_2 and $CeCoIn_5$, where K_{HF} exhibits a peak in the paramagnetic state. In $CePt_2In_7$ K_{HF} was determined via ^{195}Pt NMR in a powder sample, thus the precision was not as high as for a single crystal in which the full susceptibility tensor can be measured (13). The new results in the $CeRhIn_5$ reported here, however, were indeed acquired in a single crystal and confirm that relocalization behavior appears to be a common feature of antiferromagnetic materials.

Conclusions

We have measured the emergence of the Kondo liquid and investigated its response to long range order in several heavy fermion compounds. In the superconductors $CeCoIn_5$ and $CeIrIn_5$ as well as the hidden order compound URu_2Si_2, K_{HF} rises continuously below T^* down to the ordering temperature without saturation. In the antiferromagnets $CeRhIn_5$ and $CePt_2In_7$ the Kondo liquid relocalizes as a precursor to long-range order of partially screened local moments. Much of this behavior can be understood in the the framework of hybridization effectiveness introduced in the context of the two-fluid phenomenology (4). In this picture $K_{HF}(T) \sim f_0$, where f_0 is a measure of the collective hybridization that reduces the magnitude of the local f moments, and $f_0 = 1$ corresponds to complete hybridization. $CeCoIn_5$, $CeIrIn_5$, and URu_2Si_2 correspond to materials with $f_0 > 1$, whereas $CeRhIn_5$ and $CePt_2In_7$ have $f_0 < 1$. Although the results reported here do not directly address issues of non-Fermi liquid behavior and the presence of quantum critical phenomena in Kondo lattice systems, they do have important implications for theory (35, 36). The dual nature of the coexisting local moments and the heavy electron fluid that exists in these materials below T^* suggests that the physics cannot be described in terms of a single electronic degree of freedom. Rather, the interactions between the local moments, the heavy electron quasiparticles, and their relative spectral weight should be taken into account.

ACKNOWLEDGMENTS. We thank S. Balatsky, P. Coleman, M. Graf, D. Pines, and J. Thompson for stimulating discussions. Work at UC Davis on the URu_2Si_2 material was supported by UCOP-TR01; the work on $CePt_2In_7$ was supported by the National Nuclear Security Administration under the Stewardship Science Academic Alliances program through DOE Research Grant number DOE DE-FG52-09NA29464; the work on $CeIrIn_5$ was supported by the National Science Foundation under Grant DMR-1005393. Work in China was supported by the Chinese Academy of Sciences and NSF-China (Grant No. 11174339). Los Alamos National Laboratory is operated by Los Alamos National Security, LLC, for the National Nuclear Security Administration of the US Department of Energy under Contract DE-AC52-06NA25396.

1. Löhneysen Hv, Rosch A, Vojta M, Wölfle P (2007) Fermi-liquid instabilities at magnetic quantum phase transitions. *Rev Mod Phys* 79:1015–1075.
2. Doniach S (1977) The Kondo lattice and weak antiferromagnetism. *Physica* 91:231–234.
3. Yang Y-F, Fisk Z, Lee H-O, Thompson JD, Pines D (2008) Scaling the Kondo lattice. *Nature* 454:611–613.
4. Yang Y-F, Pines D (2012) Emergent states in heavy electron materials. *Proc Natl Acad Sci USA* 45:3060–3066.
5. Yamamoto SJ, Si Q (2007) Fermi surface and antiferromagnetism in the Kondo lattice: An asymptotically exact solution in $d > 1$ dimensions. *Phys Rev Lett* 99:016401.
6. Custers J, et al. (2003) The break-up of heavy electrons at a quantum critical point. *Nature* 424:524–527.
7. Stockert O, et al. (2004) Nature of the A phase in $CeCu_2Si_2$. *Phys Rev Lett* 92:136401.
8. Park T, Graf MJ, Boulaevskii L, Sarrao JL, Thompson JD (2008) Electronic duality in strongly correlated matter. *Proc Natl Acad Sci USA* 105:6825–6828.
9. Nakatsuji S, Pines D, Fisk Z (2004) Two fluid description of the Kondo lattice. *Phys Rev Lett* 92:016401–4.
10. Yang Y-F, Pines D (2008) Universal behavior in heavy-electron materials. *Phys Rev Lett* 100:096404.
11. Curro NJ, Young BL, Schmalian J, Pines D (2004) Scaling in the emergent behavior of heavy-electron materials. *Phys Rev B* 70:235117.
12. Yang YF, Urbano R, Curro NJ, Pines D (2009) Magnetic excitations in Kondo liquid: Superconductivity and hidden magnetic quantum critical fluctuations. *Phys Rev Lett* 103:197004.
13. Aproberts-Warren N, et al. (2011) Kondo liquid emergence and relocalization in the approach to antiferromagnetic ordering in $CePt_2In_7$. *Phys Rev B* 83:060408.
14. Clogston AM, Jaccarino V (1961) Susceptibilities and negative Knight shifts of intermetallic compounds. *Phys Rev* 121:1357–1362.
15. Abragam A (1961) *The Principles of Nuclear Magnetism* (Oxford Univ Press, Oxford).
16. Kim E, Makivic M, Cox DL (1995) Knight shift anomalies in heavy electron materials. *Phys Rev Lett* 75:2015–2018.
17. Ohama T, Yasuoka H, Mandrus D, Fisk Z, Smith JL (1995) Anomalous transferred hyperfine coupling in $CeCu_2Si_2$. *J Phys Soc Jpn* 64:2628–2635.
18. Mila F, Rice TM (1989) Spin dynamics of $YBa_2Cu_3O_{6+x}$ as revealed by NMR. *Phys Rev B* 40:11382–11385.
19. Christianson AD, et al. (2004) Crystalline electric field effects in $CeMIn_5$ (M = Co, Rh, Ir): Superconductivity and the influence of Kondo spin fluctuations. *Phys Rev B* 70:134505.
20. Curro NJ, et al. (2001) Anomalous NMR magnetic shifts in $CeCoIn_5$. *Phys Rev B* 64:180514–4.
21. Curro NJ (2011) *Encyclopedia of Magnetic Resonance*, eds RK Harris and RE Wasylishen (John Wiley, Chichester, UK).
22. Mydosh JA, Oppeneer PM (2011) Colloquium: Hidden order, superconductivity, and magnetism: The unsolved case of URu_2Si_2. *Rev Mod Phys* 83:1301–1322.
23. Wiebe CR, et al. (2007) Gapped itinerant spin excitations account for missing entropy in the hidden-order state of URu_2Si_2. *Nat Phys* 3:96–99.
24. Slichter CP (1992) *Principles of Nuclear Magnetic Resonance* (Springer, New York, Berlin, Heidelberg), 3rd ed.
25. Harrison N, Jaime M, Mydosh JA (2003) Reentrant hidden order at a metamagnetic quantum critical end point. *Phys Rev Lett* 90:096402.
26. Bernal O, et al. (2000) NMR detection of temperature-dependent magnetic inhomogeneities in URu_2Si_2. 281–282:236–237.
27. Kohori Y, Matsuda K, Kohara T (1996) ^{29}Si NMR study of antiferromagnetic superconductor URu_2Si_2. *J Phys Soc Jpn* 65:1083–1086.
28. Hanzawa K (2007) Hidden octupole order in URu_2Si_2. *J Phys Condens Matter* 19:072202.
29. Maple MB, et al. (1986) Partially gapped fermi surface in the heavy-electron superconductor URu_2Si_2. *Phys Rev Lett* 56:185–188.
30. Haraldsen JT, Dubi Y, Curro NJ, Balatsky AV (2011) Hidden-order pseudogap in URu_2Si_2. *Phys Rev B* 84:214410.
31. Llobet A, et al. (2004) Magnetic structure of $CeRhIn_5$ as a function of pressure and temperature. *Phys Rev B* 69:24403–1.
32. Hegger H, et al. (2000) Pressure-induced superconductivity in quasi-2d $CeRhIn_5$. *Phys Rev Lett* 84:4986–4989.
33. Bao W, et al. (2000) Incommensurate magnetic structure of $CeRhIn_5$. *Phys Rev B* 62: R14621–R14624.
34. Curro NJ, et al. (2003) Low-frequency spin dynamics in the $CeMIn_5$ materials. *Phys Rev Lett* 90:227202.
35. Si QM, Rabello S, Ingersent K, Smith JL (2001) Locally critical quantum phase transitions in strongly correlated metals. *Nature* 413:804–808.
36. Coleman P, Schofield AJ (2005) Quantum criticality. *Nature* 433:226–229.
37. Curro NJ (2009) Nuclear magnetic resonance in the heavy fermion superconductors. *Rep Prog Phys* 72:026502.